1. Supplemental Methods

1.1 Mice

Creation of the Tnf-KO allele: Genomic fragment containing coding regions of exons 2, 3 and 4 of the mouse *Tnf* gene were deleted using CRISPR/Cas9-mediated non homologous end joining (NHEJ). Two gRNA were designed to target the *Tnf* intron 1 (IVS1) and its 3'UTR, respectively. The gRNA target sequences within IVS1-gcaccgcagaaagaagccgt and 3'UTR-agcgggcatggtccacggag were selected for optimal specificity and cleavage using the CRISPOR online tool [1]. NHEJ events at the gRNA target sites led to the excision of the genomic fragment containing exons 2, 3 and 4 resulting in a Tnf-KO allele. Mouse genome engineering by direct Cas9/CRISPR zygote electroporation: Cas9/CRISP mediated modification of the *Tnf* sequence was carried out by electroporation of fertilized mouse oocytes essentially as previously described [2]. Frozen 1-cell stage BALB/cByJRj embryos (Janvier labs) were thawed and cultured briefly in M16 medium (Sigma). Viable embryos were selected and used immediately for electroporation. All embryo electroporations were performed using the ECM830 electroporator (BTX-Harvard Apparatus). Embryos were washed 2x in OptiMEM medium and transferred in 10 uL of OptiMEM to a 1mm gap electroporation cuvette containing 10uL of electroporation solution: 10µLOptiMEM, IVS1 and IVS2 cr:trcr gRNA duplexes (8µM each), Cas9HiFi V3 protein (IDT) (16µM). For generation of floxed allele, the solution also contained IVS1LoxP and IVS2LoxP ssODN HR templates (200 ng/µl each). Electroporation was performed with two 3ms pulses of 30V at 100ms intervals. Embryos that survived the electroporation were transferred on the same day into the oviducts of 8–16-wk-old pseudopregnant Crl: CD1 (ICR) females (0.5 d used after coitus) that had been mated with sterile genetically vasectomized males the day before embryo transfer [3]. Pregnant females were allowed to deliver and raise their pups until weaning age and founders were identified by PCR analysis of genomic DNA obtained from biopsy samples. TCRM mice were crossed with TNF-$\alpha^{-/-}$ mice to obtain haploinsufficient (**TCRM** x $Tnf^{+/-}$) mice. Further breeding was performed by crossing **TCRM** x $Tnf^{+/-}$ with $Tnf^{+/-}$ mice. TCRM (Tg(Tcra,Tcrb)562Biat) mice were kindly provided by Prof. Dr. Burkhard Ludewig.

1.2 Experimental autoimmune myocarditis

Experimental autoimmune myocarditis (EAM) was induced in 6-8 week old BALB/c mice by subcutaneous injection of 200µg of α-$MyHC_{614-634}$ peptide (Ac-RSLKLMATLFSTYASADR-OH, Caslo, Denmark) emulsified 1:1 with complete Freund's adjuvant (CFA, BD Difco, USA) at day 0 and 7. At day 21 mice were euthanized by cervical dislocation under anesthesia (intraperitoneal injection of 75 mg/kg ketamine). TCR-M were euthanized following the same procedure at age of 6 or 12 weeks and organs were harvested for histological analysis or cell isolation. For survival analysis, mice were kept in standard conditions and observed for up to 30 weeks. The animals were evaluated daily for the following symptoms: response to external stimulus, reduced physical activity, self-isolation, presence

of ruffled coat, presence of stooped posture/curved back, diarrhea, no self-cleaning/dirty coat using 0-2 scale for each parameter. Mice with the cumulative score >6, and/or with at least two symptoms in severe form and/or weight loss >30% (in the case of EAM model) were euthanized. Mice that were euthanized or died suddenly underwent autopsy and animals with visible signs of myocarditis were counted as deceased from myocarditis. All animal experiments followed the guidelines from Directive 2010/63/EU of the European Parliament on the protection of animals used for scientific purposes.

1.3 Cell cultures

T lymphocytes and antigen-presenting cells (APC) were isolated from the spleens of EAM and TCR-M mice. Briefly, single-cell suspension of splenocytes was obtained by gently smashing the spleen through 70µm and 40µm cell strainers and red blood cells were lysed using ACK lysis buffer. Suspension of splenocytes was enriched in $CD4^+$ cells using Dynabeads® Untouched™ Mouse CD4 Cells (Invitrogen, USA) according to the manufacturer's protocol. Cells were labeled with anti-CD11b-APC (1:1000, M1/70, ThermoFisher, USA),anti-CD4-PE-Cy7(1:1000, RM4-5, BioLegend, USA), anti-CD44-FITC (1:500, IM7, BioLegend) and anti-CD62L-PE (MEL-14, BioLegend) in staining buffer (2% FBS, 2mM EDTA in PBS) and incubated for 15 minutes in 4℃. Cells were FACS sorted as effector T lymphocytes (Teff) $CD4^+CD11b^-CD44^+CD62L^-$ and naïve T lymphocytes (Tn) $CD4^+CD11b^-CD44^{low}CD62L^+$. For APC isolation, the same suspension of splenocytes as used during T cells isolation was labeled using anti-CD11b-APC (1:1000, M1/70, ThermoFisher), anti-CD45-PE (30-F11, ThermoFisher), and anti-MHCII-FITC (M5/114.15.2, BioLegend) and FACS sorted as $CD45^+$, CD11b, $MHCII^+$. Cell sorting was performed using BD FACSAria II (BD Biosciences, San Jose, CA, USA). Co-cultures of T cells and APC (100 thousand/ml, ratio 10:1) and splenocytes from TCRM mice ($4x10^5$ cells/ml) were seeded in RPMI 1640 with L-glutamine (Corning, USA) supplemented with 10% fetal bovine serum (FBS, Gibco, Waltham, WA, USA), penicillin-streptomycin (1:100, Gibco) and β-mercaptoethanol (1:1000, Sigma-Aldrich, Saint Louis, USA). To activate T cells, 10ng/ml of α-MyHC was added to the medium. After 3 days of co-culture, a conditioned medium was collected and used for further experiments. Primary cardiac microvascular endothelial cells (cMVECs) were purchased from Cedarlane, Canada, and cultured in RPMI 1640 supplemented with 10% FBS. Selected experiments were performed on cMVECs isolated from hearts of 4 weeks old wild-type and $Tnf^{-/-}$ mice as described in [4]

1.4 Flow cytometry

For measurement of intracellular adhesion molecules, cultured MVECs were labeled with anti-ICAM1-PE (1:500, YN1/1.7.4, Thermo Fisher Scientific, USA), anti-VCAM1-PE-Cy7 (1:500, 429, Biolegend) anti-P-selectin-APC (1:500, RMP-1, BioLegend) and anti-CD31-FITC (1:500, 390, ThermoFisher) in staining buffer (1% FBS, 1mM EDTA in PBS). To analyze heart-infiltrating leukocytes, hearts were excised, mechanically dissected and enzymatically digested as described previously[5]. Next, cells were labeled with anti-CD3-FITC (1:250, 17A2, ThermoFisher), anti-CD4-PE-Cy7 (1:1000, RM4-5,

BioLegend), anti-CD11b-PE (1:500, M1/70, BioLegend), anti-B220-APC-Cy7(RA3-6B2, BioLegend), anti-CD49b-APC (DX5. 1:500, BioLegend) anti-CD45-BV 421 (30-F11, 1:500, BioLegend) or with anti-CD11b-PE (1:500, M1/70, BioLegend), anti-Ly6C-BV 421 (1:500, HK1.4, BioLegend), anti-Ly6G-PECy7 (1:500, 1A8-Ly6g, Invitrogen), anti-CD36-APC (1:300, HM36, Invitrogen), and anti-CD11c-PerCp (1:300, N418, BioLegend). The proliferation of T cells was measured using CellTrace™ CFSE Cell Proliferation Kit (Thermofisher). Analysis of apoptosis was performed using Annexin-V-FITC (Thermofisher) and propidium iodide (Thermofisher). All samples were suspended in flow cytometry buffer (2% FBS, 1 mM EDTA in PBS) prior to cytometric analysis. Samples were analyzed using BD FACSCanto™ II analyzer (BD Biosciences), and the data were analyzed with the FlowJo software (Tree Star, FlowJo X 10.0.7., Ashland, AS, USA).

1.5 Adhesion assay

BioFlux 200 48-well plates 0-20 dyn (Fluxion, USA) capillaries were coated with 0.4% gelatin (Merck, Germany) and 25μg/ml human fibronectin (Merck, Germany) solution in a growth medium for 24h in 37°C. MVECs suspension in growth medium ($2{,}5x10^6$ cells/ml) was loaded into capillaries using BioFlux 200 system (Fluxion, USA). Cells were grown inside capillaries until a confluent monolayer was formed. For adhesion assay, splenocytes suspension from 4 weeks old BALB/c mice labeled with CellTrace™ CFSE (ThermoFisher, USA) was used at a concentration of $3x10^5$ cells/ml. Splenocyte suspension was continuously pushed through the MVEC-coated capillaries for 30 minutes at 1dyn/cm^3 and cell adhesion was monitored with a fluorescence microscope (LS720, Etaluma, USA). The analysis of rolling parameters was performed on recorded time-lapse videos. The rolling distance was estimated on randomly chosen 50 events (start of rolling to firmly adhering) using ImageJ software (Version 1.52a, NIH, Bethesda, MA, USA).

1.6. ELISA

Levels of TNF-α, IL-6 and GM-CSF were measured in medium conditioned of T lymphocytes using ElisaMax kits (BioLegend) according to manufacturer instructions and analyzed on M200 PRO plate reader (TECAN Instruments, Switzerland). TNF-α levels in cMVECs were measured in lysates prepared using–RIPA buffer supplemented with protease inhibitors (ThermoFisher Scientific, USA). In each measurement 100μg of protein was used, protein levels were determined using Pierce™ BCA Protein Assay Kit (ThermoFisher, USA).

1.8 Histology

Mouse hearts were fixed in 4% formalin and embedded in paraffin. Standard hematoxylin/eosin staining was performed to visualize and grade the size of leukocyte infiltrates. Myocarditis severity was assessed at day 21 in EAM mice, 4 weeks old TCRM mice, and in TCRM displaying serious symptoms of health worsening. Myocarditis severity was scaled from 0 to 6 (0 = no leukocyte infiltrates; 1 = small foci of

leukocytes; 2 = larger foci of >100 inflammatory cells; 3 = more than 10% of a cross-section involved; 4 = more than 30% of a cross-section involved, 5 = more than 50% of a cross-section involved. An experienced researcher performed a blinded assessment of the histological slides. Fibrosis was visualized using Trichrome Stain (Masson) Kit (Sigma) and expressed as a percentage of the cross-sectional area involved. Cardiomyocyte hypertrophy was assessed using Wheat Germ Agglutinin, Alexa Fluor™ 488 Conjugate (Thermofisher) staining. The area of 100 randomly chosen cardiomyocytes with a visible nucleus from each heart was measured using ImageJ software and expressed as the mean area.

1.9 Echocardiography

Transthoracic echocardiography was performed using a Vevo 2100 system equipped with a 30-MHz transducer (VisualSonics). Anaesthesia was induced by 5% isoflurane and confirmed by the absence of the withdrawal reflex of one of the hind paws. During echocardiogram acquisition isoflurane was reduced to 1.5-2%. Each animal was placed in a supine position on a prewarmed platform. The limbs were taped over the metal ECG leads to enable continuous monitoring of the heart rate and respiration. Then, the prewarmed echo transmission gel was applied to the hairless chest. The heart was imaged in the bi-dimensional (2-D) mode, in the parasternal long-axis (PSLAX), short-axis (SAX) and apical 4-chamber views. For analysis of left ventricular end-diastolic volume and left the ventricular end-systolic volume the endocardium of the left ventricle was traced at both diastole and systole. An integrated software tool (LV-Trace) was used for single-plane PSLAX analysis. Collected parameters include: ejection fraction, stroke volume, left ventricular end-systolic diameter and fractional shortening.

1.10 Assessment of global cardiac function with MRI

All animals were scanned during daytime (0800 -1600), in a pseudo-random order. During the experiment, mice were anesthetized using isoflurane (1.7 vol%) in an oxygen and air (1:2) mixture. A tail-vein catheter pre-filled with heparinized saline (0.9% NaCl + 50 IU/ml Heparin) was placed to administrate pharmacological agents. Body temperature was monitored with an endorectal probe and maintained in the range of 35.5°C–36.5°C. All MR experiments were recorded with a 9.4T small animal MRI scanner (Bruker BioSpec, Ettlingen, Germany) equipped with a 1000 mT/m gradient coil with a maximum slew rate of 3500 T/m/s. A 36 mm quadrature volume coil was used for RF excitation and detection. To evaluate the global cardiac function. the bright-blood cine images were collated in 6–7 contiguous slices covering the whole ventricle volume using a flow-compensated, prospectively gated gradient-echo FLASH sequence with the following parameters: FOV 30 x 30 mm^2, acquisition matrix: 192 x 192, TE/TR = 2.3/5 ms, slice thickness = 1 mm, number of averages = 4, flip angle = 11°. Depending on the heart rate, between 22 and 24 cine frames were acquired. The filling and ejection rates of LV were obtained with a high-frame-rate, retrospectively gated cine FLASH sequence (IgFLASH) in a mid-ventricular, short-axis slice. The following acquisition parameters were used: FOV 30 x 30 mm, acquisition matrix 128 x 128, TE/TR = 1.3/4.2 ms, slice thickness = 1 mm, number of repetitions =

1200, flip angle = 11°. The data were reconstructed to 60 frames per cardiac cycle using a vendor-provided macro (ParaVision 6.0.1, Bruker BioSpin, Ettlingen, Germany). Tagged cine images were obtained using a double-gated FLASH sequence (TE/TR 1.5/4.8 ms, flip angle 11°, FOV 30 x 30 mm^2, matrix 192 x 192, slice thickness 1.0 mm, 16 repetitions, 20–25 frames) with a spatial modulation of magnetization (SPAMM) module for tag generation (square tags: line thickness 0.2 mm, span 0.6 mm). Cardiac reserve was estimated with the same sequence as for high-frame-rate LV function with 300 repetitions and reconstruction to 30 frames2. Dobutamine hydrochloride (Sigma-Aldrich) was dissolved in 0.9% NaCl at concertation of 0.5 mg/ml and injected i.p. at a dose of 2 mg/kg (typical bolus volume ~ 100 ul)

2. Supplemental Figures

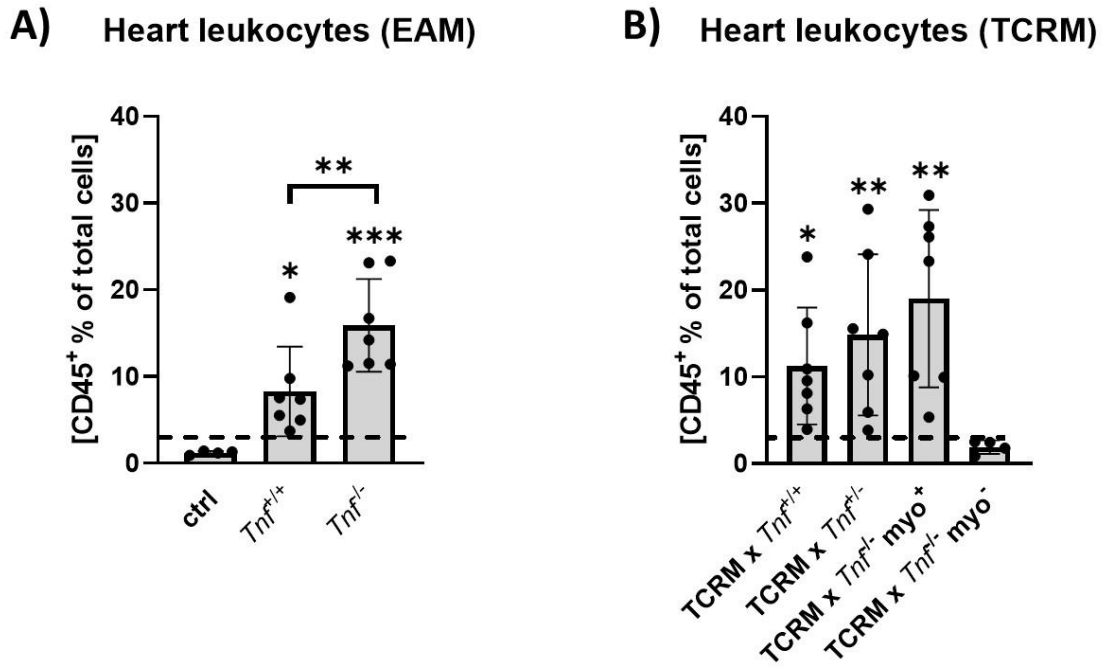

Supplementary Figure 1. Flow cytometry analysis of leukocytes in hearts from EAM and TCRM models. Panel (**A**) shows the percentage of $CD45^+$ leukocytes in the heart of healthy wild-type mice (ctrl) and immunized wild-type ($Tnf^{+/+}$) and myocarditis-positive TNF-α deficient ($Tnf^{-/-}$) mice at d19 from immunization. In panel (**B**) analysis of 6-weeks old hearts of TCRM (TCRM x $Tnf^{+/+}$), TNF-α haploinsufficient TCRM (TCRM x $Tnf^{+/-}$) and TNF-α deficient TCRM (TCRM x $Tnf^{-/-}$) is presented. TCRM x $Tnf^{-/-}$ mice were split into myocarditis positive (myo^+) and myocarditis negative (myo^-) groups. A threshold discriminating myocarditis-positive and myocarditis-negative hearts is indicated by a dotted line at 3% of $CD45^+$ cells. *p* values calculated with Kruskal-Wallis followed by Dunn's test against ctrl in (A) and one-way ANOVA followed by multiple comparison using the Fisher's LSD test against TCRM x $Tnf^{-/-}$ myo^- in (B). ns $p>0.05$, *$p<0.05$, ** $p<0.01$, *** $p<0.001$.

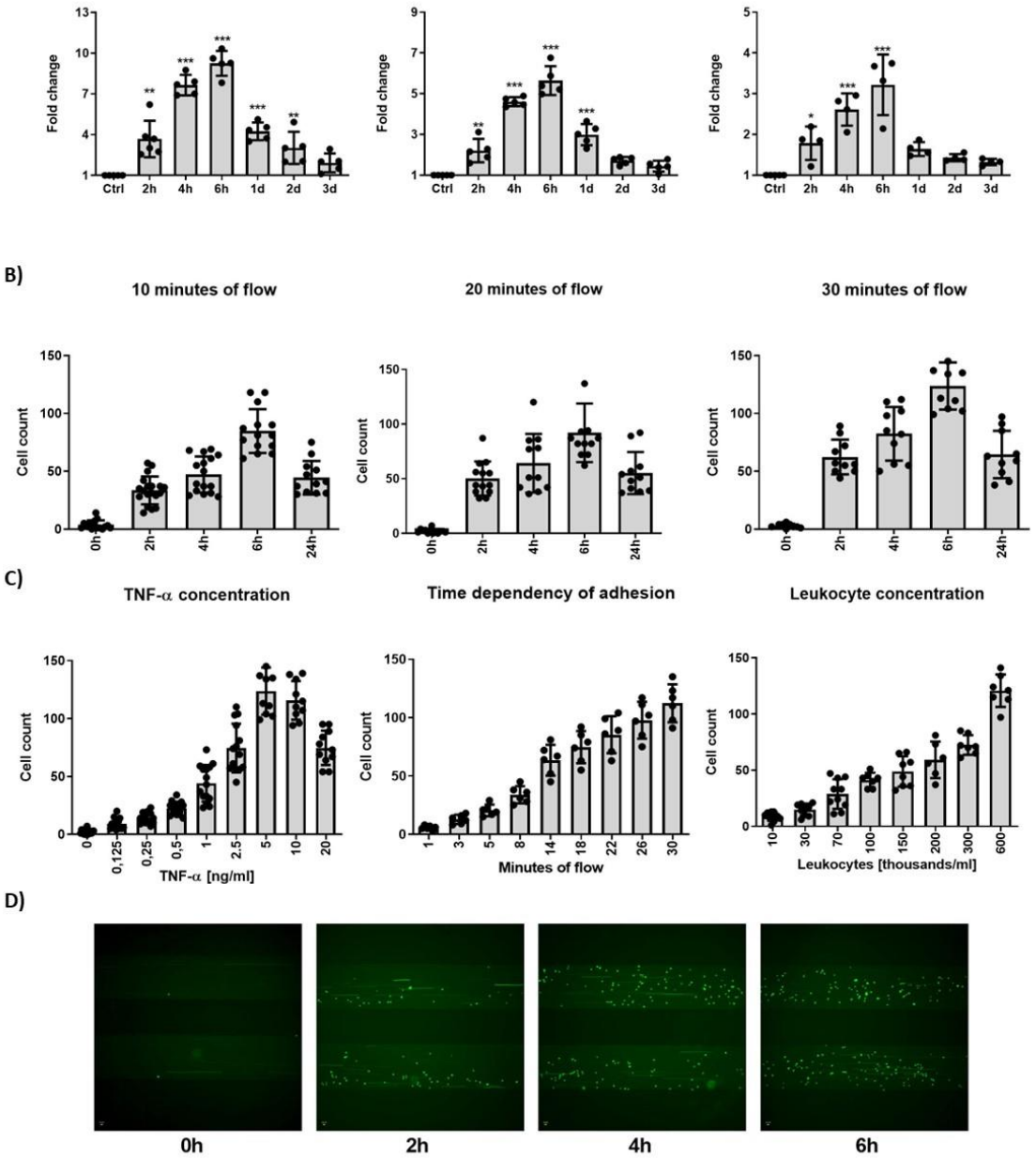

163

164 **Supplementary Figure 2.** Endothelial activation by TNF-α. cMVECs were stimulated with 5ng/ml
165 TNF-α for up to 3 days and surface expression levels of ICAM-1, VCAM-1 and p-selectin are shown in
166 panel **(A)**. Panel **(B)** demonstrates the time-dependency of TNF-α stimulation (5ng/ml) on the number
167 of leukocytes binding to cMVECs in shear flow conditions and representative microphotographs of each
168 timepoint are presented in **(C)**. Panel **(D)** shows the dependency of leukocyte adhesion on the
169 concentration of TNF-α used during stimulation, duration of the experiment and concentration of
170 leukocytes used in the experiment. *p<0.05, ** p<0.01, *** p <0.001 calculated by one-way ANOVA
171 followed by Fisher's LSD post-hoc test versus the control group.

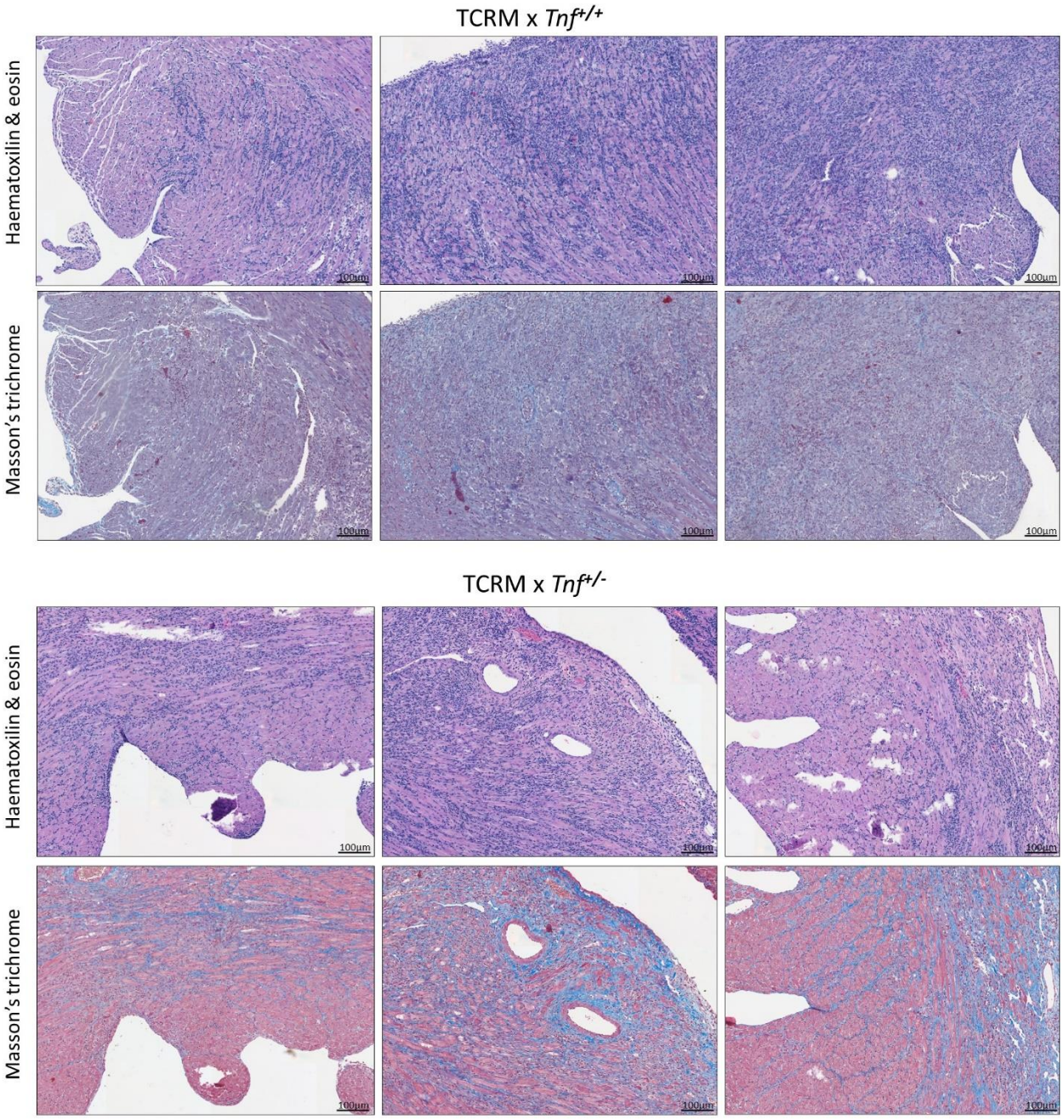

Supplementary Figure 3. Co-occurrence of inflammation and fibrosis in the TCRM model. The panel shows representative haematoxylin and eosin and Masson's trichrome staining (where blue indicates collagen deposition) for TCRM x $Tnf^{+/+}$ (inflammation without fibrosis) and TCRM x $Tnf^{+/-}$ (inflammation with fibrosis) on constitutive heart sections.

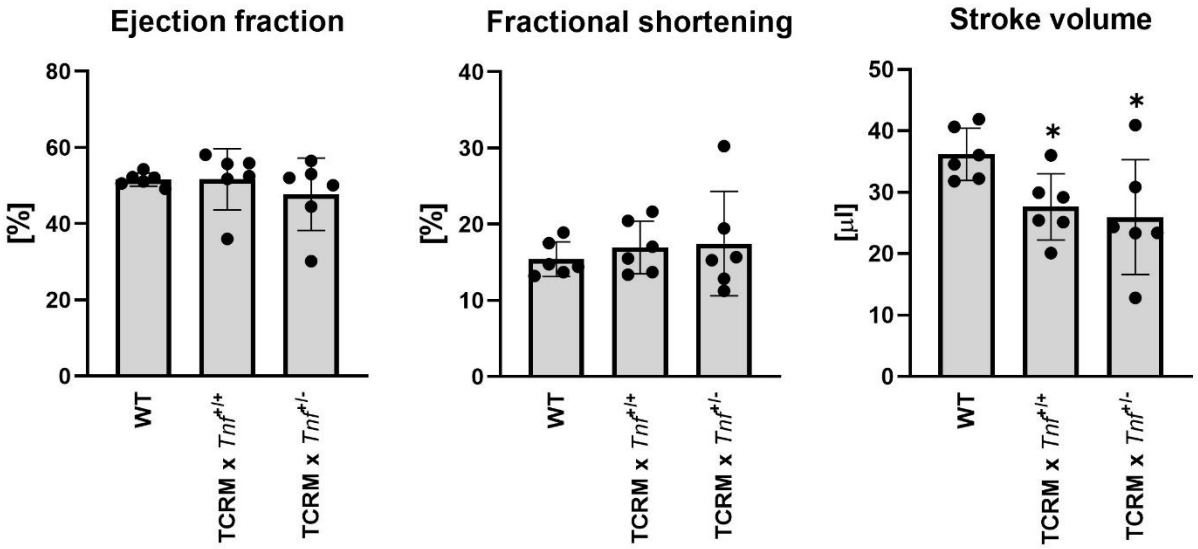

177

178 **Supplementary Figure 4.** Echocardiography of cardiac functions in 6-weeks old TCRM mice. The
179 analysis included sex-matched wild-type (WT), TCRM (TCRM x $Tnf^{+/+}$) and TNF-α haploinsufficient
180 TCRM (TCRM x $Tnf^{+/-}$) mice. The mean values of ejection fraction, fractional shortening and stroke
181 volume are presented. *p<0.05, ** p<0.01, *** p <0.001 calculated by one-way ANOVA followed by
182 multiple comparison using Fisher's LSD test

183

184

185

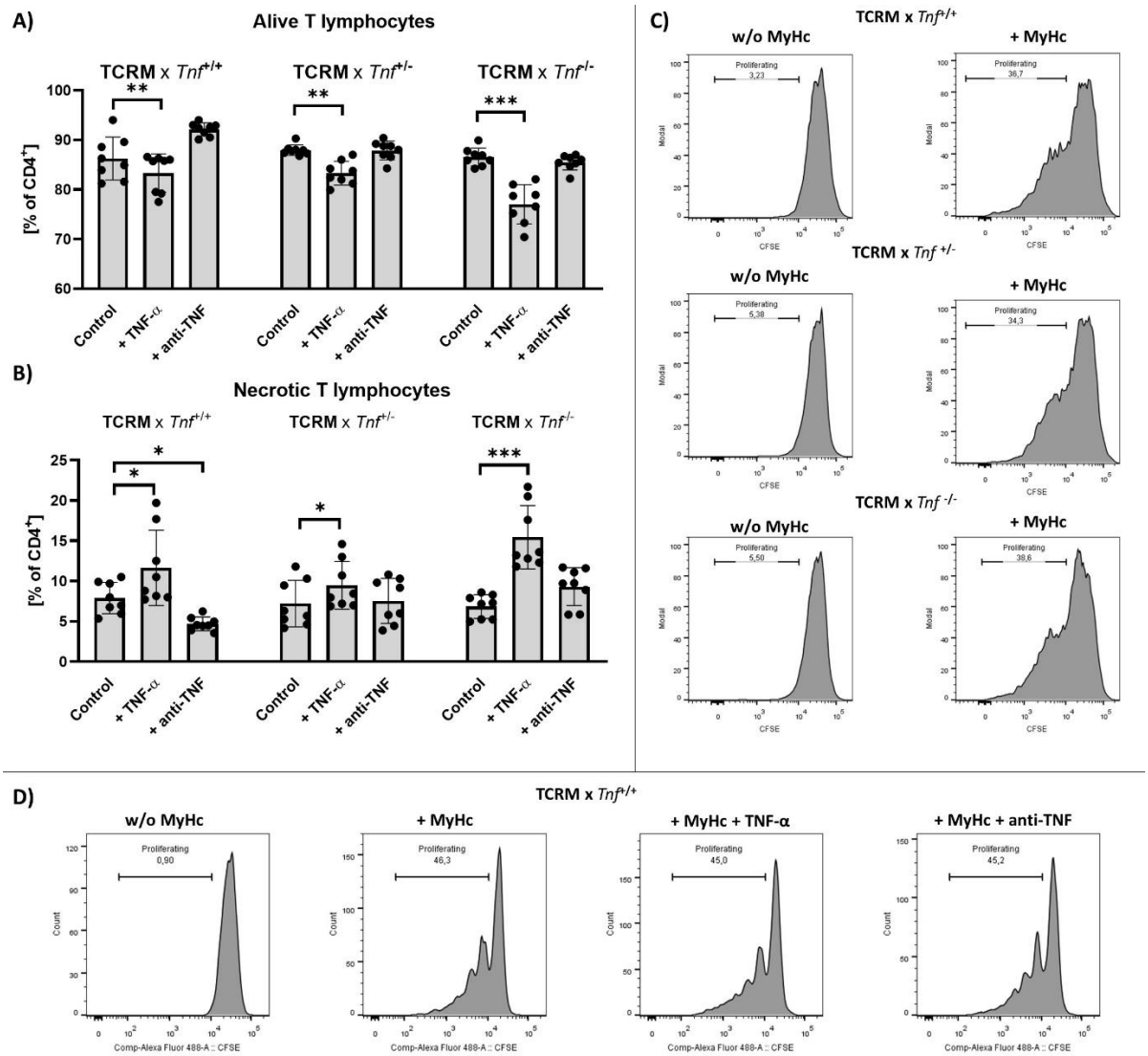

Supplementary Figure 5. Proliferation and survival of T lymphocytes from TCRM model. Splenocytes were isolated from 6 weeks old wildtype (**TCRM** x *Tnf*$^{+/+}$), haploinsufficient (**TCRM** x *Tnf*$^{+/-}$) and deficient in TNF-α (**TCRM** x *Tnf*$^{-/-}$) TCRM mice. In panels **(A)** and **(B)** T cells and APC were co-cultured for 3 days in the presence of α-MyHc peptide alone (control), with the peptide and 5 ng/ml TNF-α (+TNF-α) or the peptide and 10µg/ml of TNF-α neutralizing antibody (+ anti-TNF). Cells were stained with propidium iodide and Annexin V to determine viability, n=8. In panel **(C)** representative histograms showing proliferation of T lymphocytes co-cultured with APCs in the presence or absence of α-MyHc peptide. Panel **(D)** shows representative proliferation of T lymphocytes from **TCRM** x *Tnf*$^{+/+}$ mice in response to 5 ng/ml TNF-α (+TNF-α) or 10 µg/ml of TNF-α neutralizing antibody (+ anti-TNF) treatment. *p<0.05, ** p<0.01, *** p <0.001 calculated by one-way ANOVA followed by multiple comparison using Fisher's LSD test

A)

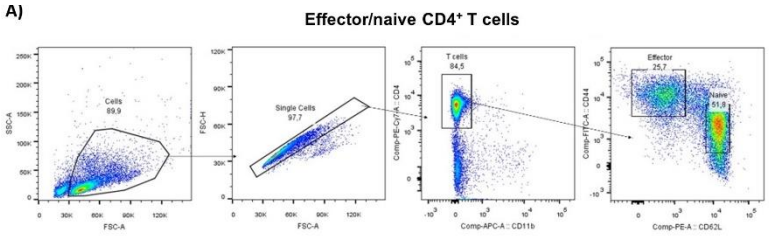
Effector/naive CD4+ T cells
Cells
89,9
Single Cells
97,7
T cells
84,5
Effector
25,7
Naive
51,8
SSC-A
FSC-A
FSC-H
Comp-PE-Cy7-A :: CD4
Comp-APC-A :: CD11b
Comp-FITC-A :: CD44
Comp-PE-A :: CD62L

B)

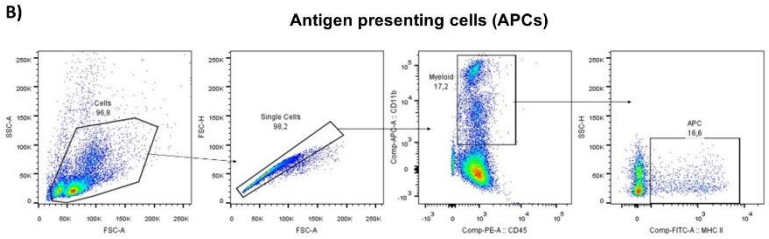
Antigen presenting cells (APCs)
Cells
96,8
Single Cells
98,2
Myeloid
17,2
APC
16,6
SSC-A
FSC-A
FSC-H
Comp-APC-A :: CD11b
Comp-PE-A :: CD45
SSC-H
Comp-FITC-A :: MHC II

C)

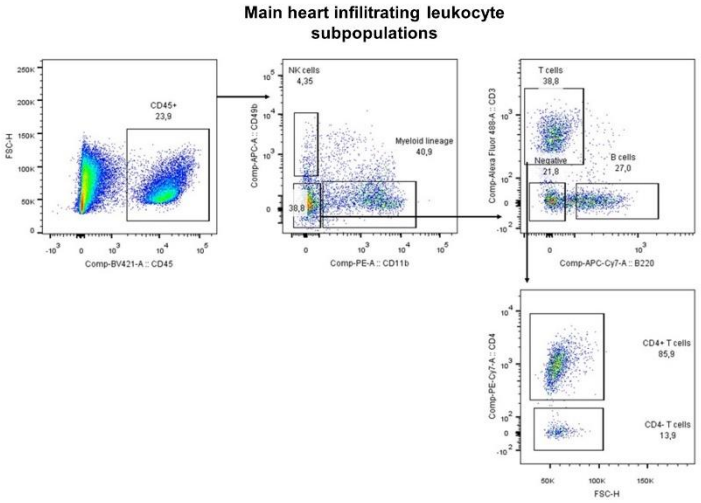
Main heart infilitrating leukocyte subpopulations
CD45+
23,9
NK cells
4,35
Myeloid lineage
40,9
38,8
T cells
39,8
Negative
21,8
B cells
27,0
CD4+ T cells
85,9
CD4- T cells
13,9
FSC-H
Comp-BV421-A :: CD45
Comp-APC-A :: CD49b
Comp-PE-A :: CD11b
Comp-Alexa Fluor 488-A :: CD3
Comp-APC-Cy7-A :: B220
Comp-PE-Cy7-A :: CD4

D)

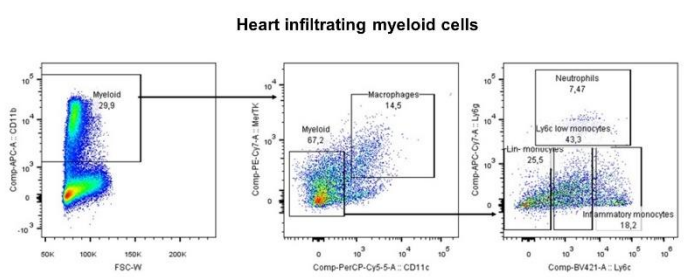
Heart infiltrating myeloid cells
Myeloid
29,9
Macrophages
14,5
Myeloid
67,2
Neutrophils
7,47
Ly6c low monocytes
43,3
Lin- monocytes
25,5
Inflammatory monocytes
18,2
Comp-APC-A :: CD11b
FSC-W
Comp-PE-Cy7-A :: MerTk
Comp-PerCP-Cy5-5-A :: CD11c
Comp-APC-Cy7-A :: Ly6g
Comp-BV421-A :: Ly6c

E)

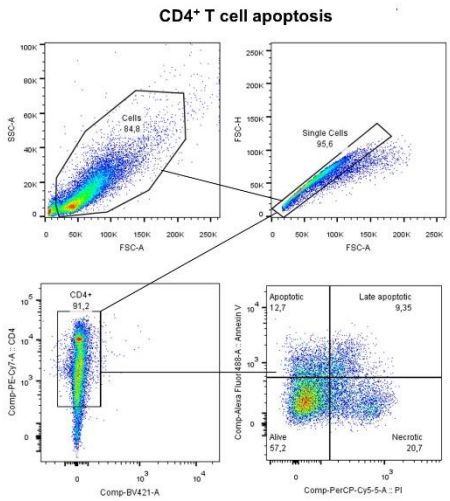
CD4+ T cell apoptosis
Cells
84,8
Single Cells
95,6
CD4+
81,2
Apoptotic
12,7
Late apoptotic
9,35
Alive
57,2
Necrotic
20,7
SSC-A
FSC-A
FSC-H
Comp-PE-Cy7-A :: CD4
Comp-BV421-A
Comp-Alexa Fluor 488-A :: Annexin V
Comp-PerCP-Cy5-5-A :: PI

Supplementary figure 6. Gating strategy used for the FACS and flow cytometry analysis. **A)** Naïve and effector T cells gating strategy used in FACS and analysis, **B)** gating strategy used for FACS of antigen-presenting cells, **C)** gating strategy used in the analysis of main subsets of heart infiltrating leukocytes and T cell subpopulations, **D)** gating strategy used in the analysis of heart infiltrating subsets of the myeloid lineage, **E)** gating strategy used for the determination of T cell activation-induced cell death (AICD).

1. Concordet JP, Haeussler M. CRISPOR: Intuitive guide selection for CRISPR/Cas9 genome editing experiments and screens. *Nucleic Acids Res*; 2018;**46**:W242–W245.

2. Wang J, Thingholm LB, Skiecevičie J, Rausch P, Kummen M, Hov JR, Degenhardt F, Heinsen FA, Rühlemann MC, Szymczak S, Holm K, Esko T, Sun J, Pricop-Jeckstadt M, Al-Dury S, Bohov P, Bethune J, Sommer F, Ellinghaus D, Berge RK, Hübenthal M, Koch M, Schwarz K, Rimbach G, Hübbe P, Pan WH, Sheibani-Tezerji R, Häsler R, Rosenstiel P, D'Amato M, et al. Genome-wide association analysis identifies variation in Vitamin D receptor and other host factors influencing the gut microbiota. *Nat Gen*; 2016;**48**:1396–1406.

3. Haueter S, Kawasumi M, Asner I, Brykczynska U, Cinelli P, Moisyadi S, Bürki K, Peters AHFM, Pelczar P. Genetic vasectomy - Overexpression of Prm1-EGFP fusion protein in elongating spermatids causes dominant male sterility in mice. *Genesis*; 2010;**48**:151–160.

4. Rolski F, Czepiel M, Tkacz K, Fryt K, Siedlar M, Kania G. T Lymphocyte-Derived Exosomes Transport MEK1 / 2 and ERK1 / 2 and Induce NOX4-Dependent Oxidative Stress in Cardiac Microvascular Endothelial Cells. *Oxid Med Cell Longev* 2022;**2022**:1–17.

5. Tkacz K, Rolski F, Czepiel M, Działo E, Siedlar M, Eriksson U, Kania G, Błyszczuk P. Haploinsufficient Rock1+/− and Rock2+/− Mice Are Not Protected from Cardiac Inflammation and Postinflammatory Fibrosis in Experimental Autoimmune Myocarditis. *Cells* 2020;**9**:700.